European Journal of Medicinal Chemistry 45 (2010) 1068–1077

Contents lists available at ScienceDirect

European Journal of Medicinal Chemistry

journal homepage: http://www.elsevier.com/locate/ejmech

Original article

Synthesis of new spiroindolinones incorporating a benzothiazole moiety as antioxidant agents

Nilgün Karalı [a], Özlen Güzel [a,*], Nurten Özsoy [b], Süheyla Özbey [c], Aydın Salman [a]

[a] Istanbul University, Faculty of Pharmacy, Department of Pharmaceutical Chemistry, 34116 Beyazıt, Istanbul, Turkey
[b] Istanbul University, Faculty of Pharmacy, Department of Biochemistry, 34116 Beyazıt, Istanbul, Turkey
[c] Hacettepe University, Department of Physics Engineering, 06532 Beytepe, Ankara, Turkey

ARTICLE INFO

Article history:
Received 3 August 2009
Received in revised form
30 November 2009
Accepted 2 December 2009
Available online 21 December 2009

Keywords:
3-Spiroindolinone
Benzothiazole
Synthesis
X-ray analyses
Antioxidant activity
Cytotoxicity

ABSTRACT

3*H*-Spiro[1,3-benzothiazole-2,3′-indol]-2′(1′*H*)-ones **3a–c** and **4a–e** were synthesized from treating the 5-substituted 1*H*-indole-2,3-diones with 2-aminothiophenol in ethanol. The structures were confirmed by elemental analyses, spectrometry (IR, ^{1}H NMR, ^{13}C NMR, HSQC-2D and LCMS-APCI) and single crystal X-ray analysis. The new compounds were screened for their antioxidant activities such as the Fe^{3+}/ascorbate system induced inhibition of lipid peroxidation (LP) in liposomes, trolox equivalent antioxidant capacity (TEAC), scavenging effect on diphenylpicryl hydrazine (DPPH$^{\bullet}$), and reducing power. These compounds showed potent scavenging activities against DPPH$^{\bullet}$ and 2,2′-azino-bis(3-ethylbenzthiazoline-6-sulphonic acid) ($ABTS^{\bullet+}$) radicals, reducing powers, and strong inhibitory capacity on lipid peroxidation. Compound **4a** incorporating methyl both at R_1 and R_2 was found to be the most potent antioxidant described in this study. Compounds **3b** and **4b** were selected as representative compounds by the National Cancer Institute for screening against anticancer activity and these compounds were found to be cytotoxic against CNS cancer cell line SNB-75 in the primary screen.

1. Introduction

Antioxidants have gained a lot of importance because of their potential as prophylactic and therapeutic agents in many diseases. Free radicals are constantly formed as a result of normal organ functions or excessive oxidative stress [1]. High levels of free radicals can cause damage to biomolecules such as lipids, proteins, enzymes and DNA in cells and tissues, resulting in mutations that can lead to malignancy. Damage to DNA by oxidative stress has been widely accepted as a major cause of cancer [2]. DNA mutation is a critical step in carcinogenesis and elevated levels of oxidative DNA lesions have been observed in various tumours. The discovery of the role of free radicals in cancer, diabetes, cardiovascular diseases, autoimmune diseases, neurodegenerative disorders, aging and other diseases has led to new medical insight [3,4]. Minimizing oxidative damage may be an important approach to the primary prevention or treatment of these diseases, since antioxidants may stop the free-radical formation, or interrupt an oxidizing chain reaction. This had attracted a great deal of research interest in therapeutic antioxidant-based drugs formulations. The development of synthetic compounds, capable of scavenging free radicals, has been a great success.

In recent years, many publications have covered the antioxidant and cytotoxic roles of several indole derivatives. The antioxidant behaviour of a series of substituted indoline-2-ones and indoline-2-thiones was investigated using an oxygen radical absorbance capacity assay. The results indicated that the examined indoline derivatives had effective activities as radical scavengers [5]. Some indole-3-carboxamides were potent inhibitors of superoxide anion formation [6,7]. Several benzimidazole containing indole derivatives showed very good *in vitro* free-radical scavenging properties as shown by determination of their scavenge superoxide anion formation capacity [8]. Phytoalexins are secondary metabolites produced by certain plants in response to pathogen attack or various forms of stress. Indole phytoalexins from cruciferous plants, such as brassinin, spirobrassinin, 1-methoxyspirobrassinol and camalexin demonstrate *in vivo* cytostatic/cytotoxic effects against cultured human solid tumour and leukemia cell lines [9,10]. Synthetic 2-amino analogs of 1-methoxyspirobrassinol were found to be significantly cytotoxic against human cancer cell lines (Fig. 1) [11,12].

Abbreviations: ABTS, 2,2′-azino-bis(3-ethylbenzthiazoline-6-sulphonic acid); BHT, butylated hydroxytoluene; CNS, central nervous system; DMF, dimethylformamide; DMSO, dimethyl sulfoxide; DPPH, diphenylpicryl-hydrazine; EC50, effective concentration 50%; GI, growth inhibition; LP, lipid peroxidation; MDA, malondialdehyde; NSCL, non-small cell lung; ROS, reactive oxygen species; SD, standard deviation; SRB, sulphorhodamine B; TBA, thiobarbituric acid; TBARS, thiobarbituric acid reactive substances; TCA, trichloroacetic acid; TEAC, trolox equivalent antioxidant capacity; TRAP, total radical antioxidant potential.

* Corresponding author. Tel.: +90 212 4400000; fax: +90 212 4400252.
E-mail address: ozlen_guzel@yahoo.com (Ö. Güzel).

0223-5234/$ – see front matter © 2009 Elsevier Masson SAS. All rights reserved.
doi:10.1016/j.ejmech.2009.12.001

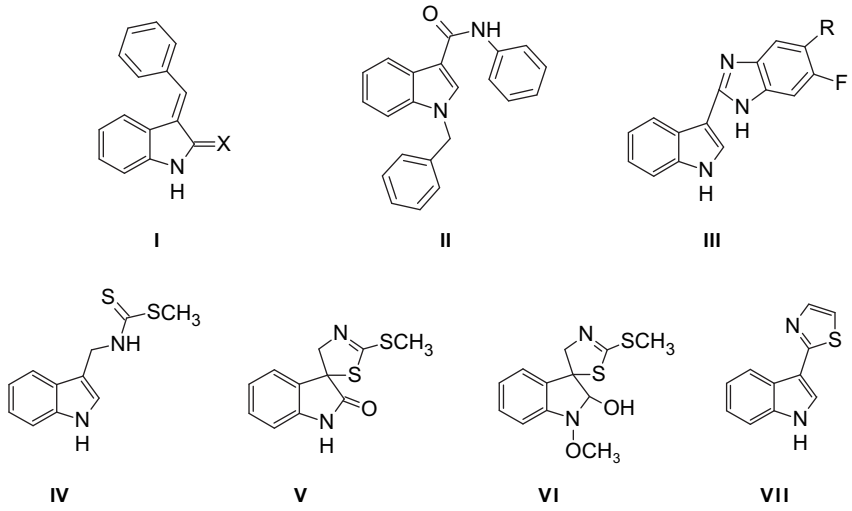

Fig. 1. Structures of indoline-2-ones/thiones (**I**), indole-3-carboxamides (**II**), indolilbenzimidazoles (**III**), brassinin (**IV**), spirobrassinin (**V**), 1-methoxybrassinol (**VI**) and camalexin (**VII**).

A large number of 2-arylbenzothiazoles have been prepared because of their wide pharmacological potency, i.e. significant anticancer [13–15] and antioxidant properties [16,17]. 2-Arylbenzothiazoles are most commonly synthesized by the condensation of 2-aminothiophenols with substituted aldehydes, carboxylic acids, acyl chlorides, and nitriles [18,19]. The reactivity of 1*H*-indole-2,3-diones towards 2-aminothiophenol has been the subject of a number of reports and some of the products obtained are quite interesting. The first results reported that 1*H*-indole-2,3-dione furnished benzothiazinone, indolobenzothiazide and spirobenzothiazole when the reaction was carried out in dry xylene in the presence of anhydrous zinc chloride under reflux. On the other hand, the reaction of 1-methyl-1*H*-indole-2,3-dione with 2-aminothiophenol under the same conditions furnished solely the spiro compound (Fig. 2) [20–22]. In addition, there is one report on the reaction of 1*H*-indole-2,3-dione with 2-aminothiophenol in ethanol yielding a single spirobenzothiazole [23].

Intrigued by the above observations and in continuation of our study on indolinone derivatives, we synthesized some new spiroindolinone derivatives by incorporating the benzothiazole moiety. We investigated the antioxidant properties of indole derivatives in order to evaluate their medicinal value and to point to an antioxidant agent that could be used in pharmaceutical industry, i.e. antioxidant effect on the Fe^{3+}/ascorbate-induced lipid peroxidation in a liposome model system, TEAC, scavenging effect on DPPH$^{\bullet}$ radical, and reducing power.

2. Results and discussion

2.1. Chemistry

3*H*-Spiro[1,3-benzothiazole-2,3′-indol]-2′(1′*H*)-ones **3a–c** and 1′-methyl-3*H*-spiro[1,3-benzothiazole-2,3′-indol]-2′(1′*H*)-ones **4a–e** were synthesized from treatment of 2-aminothiophenol with 5-substituted 1*H*-indole-2,3-diones **1** or 5-substituted 1-methyl-1*H*-indole-2,3-diones **2** (Fig. 3). The structures of **3** and **4** were confirmed by elemental analyses, spectrometry (IR, ^{1}H NMR, ^{13}C NMR, HSQC-2D and LCMS-APCI) and single crystal X-ray analysis.

IR spectra of spiroindolinones **3** and **4** showed absorption bands in the 3354–3299 and 1732–1696 cm^{-1} regions resulting from the NH and C=O functions, respectively [23–25]. ^{1}H NMR spectra of **3a–c** displayed the NH protons of the indole (δ 10.01–11.07 ppm) and benzothiazole (δ 7.22–7.33 ppm) rings as two separate signals, whereas, the benzothiazole NH (δ 7.18–7.28 ppm) and the indole N-CH_3 (δ 3.08–3.20 ppm) signal were observed in the spectra of **4a–e** [23,24,26–28]. The formation of spiroindolinones is evident by both the presence of a signal assigned to spiro C (δ 74.10–74.80 ppm) and a signal attributed to the C=O function of indolinones (δ 174.75–175.62 ppm) in the ^{13}C NMR spectra of **4a–e** [28]. Further verification was obtained from the HSQC spectra of **4a–e**, which clearly show the ^{1}H–^{13}C connections and allow definite assignment of the ^{1}H and ^{13}C resonances [25,29–31]. LCMS-APCI of **3a**, **3b**, and **4b**

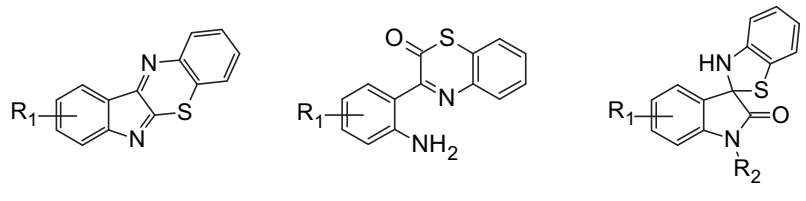

R_1= H, 5-F, 6-F

R_2= H, CH_3

Fig. 2. Structures of benzothiazinone (**VIII**), indolobenzothiazide (**IX**) and spirobenzothiazole (**X**).

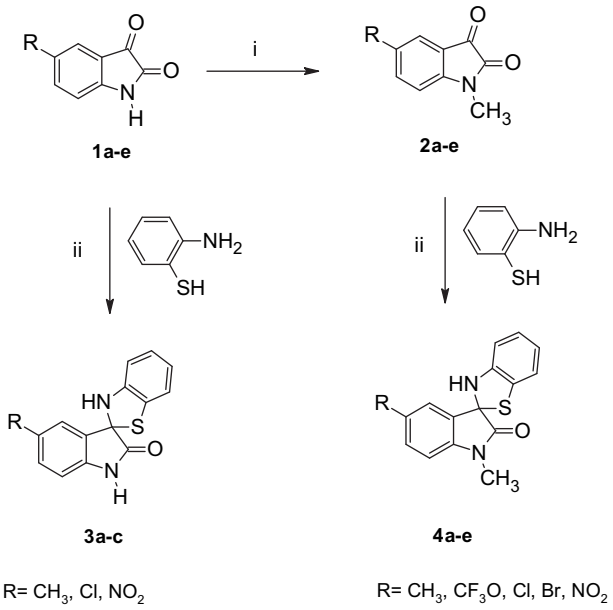

Fig. 3. Synthesis of **2**, **3** and **4**. Reagent and condition: i) NaH, anhyd. DMF, stirred, 0.5 h, CH_3I, reflux, 4 h, ii) EtOH, reflux, 5 h.

were selected as prototypes and displayed molecular ions with different intensities.

The X-ray structure of **4d** was determined in order to confirm the assigned structures and to establish conformations of the molecule. Table 1 summarizes the crystal and experimental data. Selected bond lengths and angles are listed in Table 2. The molecular structure of **4d** is shown in Fig. 4. The molecule is in its spiro form and it is not planar. The dihedral angle between the indole and benzothiazole moieties is 84.9(2)°. Based on the puckering-parameters values [32], the benzothiazole ring at C2 is twisted around the S1–C2 bond. Bond lengths and angles have normal values.

Table 1
Crystal data and structure refinement parameters for compound **4d**.

Crystal formula	$C_{15}H_{11}N_2OSBr$
Formula weight	347.23
Crystal dimensions [mm]	0.71 × 0.49 × 0.29
Temp [K]	293(2)
Crystal system	Trigonal
Space group	R-3
a [Å]	26.7410(9)
b [Å]	26.7410(9)
c [Å]	10.1420(3)
α [°]	90.0
β [°]	90.0
γ [°]	120.0
V [Å^3]	6280.7(4)
λ (MoK$_\alpha$) (Å)	0.71073
Z	18
D_{calc} [g cm^{-3}]	1.652
F(000)	3132
θ range for data collection [°]	1.52/25.6
μ (MoKα)[mm^{-1}]	3.09
Number of reflections collected	7792 (4892 I > 4σ(I))
Number of unique reflections	2728 (1651 used in refinement)
No. of refined parameters	186
R/R_w values	0.0382/0.0969
GOF	1.045
Final shift	0.001
$(\Delta\rho)_{min}$, $(\Delta\rho)_{max}$ (eÅ^{-3})	0.216, −0.226
Measurement	STOE IPDS 2 diffractometer
Structure determination	Direct methods (SHELXS-97) [37]
Refinement	Full-matrix least-squares (SHEXL-97) [38]

Table 2
Selected bond lengths and angles of compound **4d**.

Bond lengths (Å)	
Br1–C5	1.890 (4)
S1–C10	1.760 (4)
S1–C2	1.866 (6)
N2–C15	1.407 (6)
N2–C2	1.449 (5)
N1–C1	1.359 (5)
N1–C8	1.406 (5)
N1–C9	1.446 (6)
O1–C1	1.213 (4)
C3–C2	1.504 (5)
C6–C7	1.384 (6)
C1–C2	1.549 (6)
Bond angles (°)	
C10–S1–C2	90.1 (2)
C15–N2–C2	112.6 (4)
C1–N1–C8	111.4 (3)
C1–N1–C9	124.7 (3)
C15–C10–S1	112.2 (4)
C10–C15–N2	115.8 (3)
C6–C5–Br1	119.4 (3)
C3–C8–N1	110.0 (3)
C8–C3–C2	108.4 (3)
C5–C6–C7	121.0 (4)
O1–C1–N1	125.8 (4)
O1–C1–C2	126.5 (4)
N1–C1–C2	107.6 (3)
N2–C2–C3	115.3 (3)
N2–C2–C1	112.1 (4)
C3–C2–C1	102.4 (3)
N2–C2–S1	107.4 (3)

The molecular packing is shown in Fig. 5. The molecules in the crystal are packed at normal van der Waals distances. There is only one N–H···O intermolecular interaction that is smaller than 3.4 Å which helps to stabilize the molecules in the crystal, i.e. N2···O1 (x − y, x, 1 − z 1) 3.019(6) Å.

2.2. Antioxidant activity

The antioxidant activities of spiroindolinones were determined as an index of pharmacological usefulness. Four model systems were used, namely inhibition of the Fe^{3+}–ascorbate induced phospholipid degradation, DPPH$^{\bullet}$ and ABTS$^{\bullet+}$ radical scavenging, and Fe (III) reduction. In the assessment of antioxidant activity, both

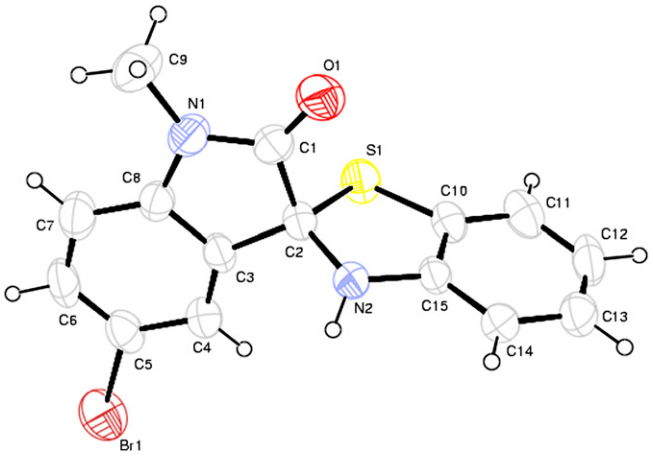

Fig. 4. Molecular structure of **4d** showing the atom labelling scheme. Displacement ellipsoids are drawn as 50% probability level.

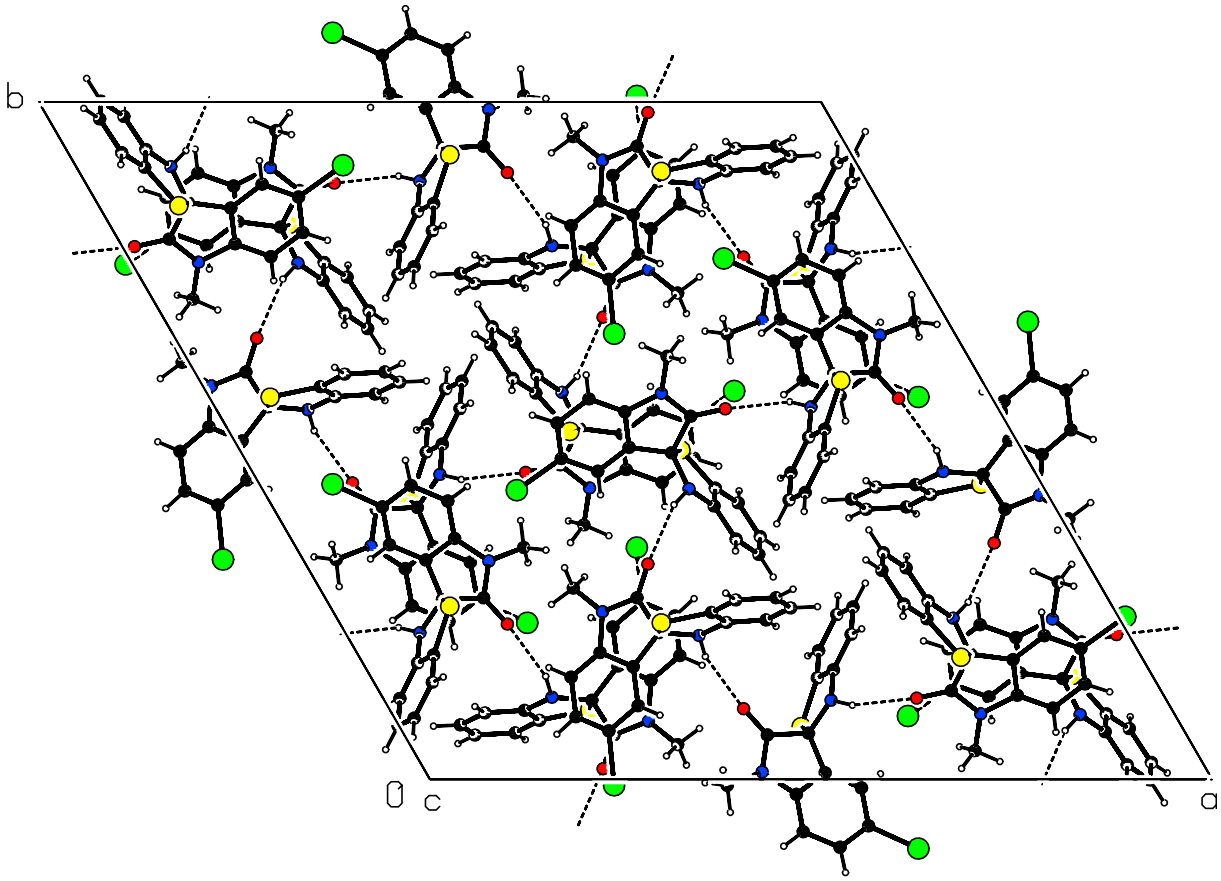

Fig. 5. Crystal packing of **4d** projected onto ab plane. The dashed lines indicated the intermolecular hydrogen bonds.

synthetic and biologically relevant free radicals were used. The synthetic nitrogen-centered DPPH$^{\bullet}$ and ABTS$^{\bullet+}$ radicals are not biologically relevant, but are often used as indicator compounds in testing hydrogen transfer capacity that are related to the antioxidant activity. The antioxidant properties were expressed as EC_{50} values (Table 3).

2.2.1. Antioxidant activity on liposome peroxidation

A well-recognized result of oxidant injury is peroxidation of membrane lipids to organic peroxyl radicals, which initiates a chain reaction that may explain many membrane-mediated effects of reactive oxygen species (ROS). The concentration-dependent inhibitory effects of indole derivatives (**3a–c** and **4a–e)** on LP in

Table 3
EC_{50} values of **3a–c** and **4a–e** in antioxidant properties.

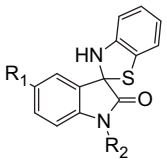

EC_{50} (mM)						
Compound	R_1	R_2	Anti-LP	DPPH	ABTS	Reducing Power
3a	CH_3	H	0.041 ± 0.001^{a}	1.30 ± 0.13^{a}	1.02 ± 0.01^{a}	1.36 ± 0.13^{a}
3b	Cl	H	0.049 ± 0.004^{a}	1.78 ± 0.06^{b}	1.03 ± 0.05^{a}	0.51 ± 0.11^{b}
3c	NO_2	H	0.087 ± 0.001^{c}	1.30 ± 0.10^{a}	1.63 ± 0.04^{c}	$0.80 \pm 0.05^{d,e}$
4a	CH_3	CH_3	0.034 ± 0.001^{d}	0.98 ± 0.14^{a}	0.98 ± 0.14^{a}	$0.70 \pm 0.17^{b,e}$
4b	CF_3O	CH_3	0.084 ± 0.004^{c}	1.62 ± 0.06^{b}	1.37 ± 0.05^{d}	4.94 ± 0.06^{f}
4c	Cl	CH_3	0.075 ± 0.002^{c}	1.24 ± 0.11^{a}	$1.14 \pm 0.14^{a,e}$	4.02 ± 0.15^{c}
4d	Br	CH_3	0.034 ± 0.002^{d}	1.01 ± 0.15^{a}	1.04 ± 0.11^{a}	4.22 ± 0.02^{c}
4e	NO_2	CH_3	0.092 ± 0.001^{c}	1.27 ± 0.15^{a}	1.34 ± 0.04^{d}	5.14 ± 0.38^{f}
Ascorbic acid			–	0.36 ± 0.04^{d}	1.20 ± 0.03^{e}	0.65 ± 0.10^{g}
α-Tocopherol			0.153 ± 0.001^{e}	0.35 ± 0.07^{d}	1.20 ± 0.01^{e}	1.95 ± 0.04^{a}

EC_{50} value: The effective concentration at which the antioxidant activity was 50%; DPPH$^{\bullet}$ and ABTS$^{\bullet+}$ radicals were scavenged by 50%, respectively, and the absorbance was 0.5 for reducing power. EC_{50} values were obtained by interpolation from linear regression analysis. Values were the means of three replicates ± SD. Values with different letters in the same column were significantly ($p < 0.05$) different.

liposomes were estimated by the amount of thiobarbituric acid reactive substances (TBARS). α-Tocopherol was used as reference antioxidant. α-Tocopherol is the most important lipophilic radical chain-breaking antioxidant in living organism. As can be seen in Table 3, the whole of the tested compounds exhibit potent inhibitory effect on the Fe^{3+}/ascorbic acid-induced LP, which is almost 2–4 times higher than that of α-tocopherol (0.153 ± 0.01 mM). Based on the EC50 values (effective concentration at which TBARS were reduced to 50% with respect to controls), R_1-methyl substituted compound **4a** and R_1-brome substituted compound **4d** incorporating methyl at R_2 were significantly ($p < 0.05$) better inhibitors than other indole derivatives. The EC_{50} values were 0.034 ± 0.001 and 0.034 ± 0.002 mM, for **4a** and **4d**, respectively. R_1-methyl substituted **3a** and R_1-chlorine substituted **3b** were the next most effective indole derivatives with EC_{50} values of 0.041 ± 0.001 and 0.049 ± 0.004 mM ($p < 0.05$), followed by R_1-chlorine substituted **4c** and R_1-trifluoromethoxy substituted **4b** with EC_{50} values of 0.075 ± 0.002 and 0.084 ± 0.004 mM ($p < 0.05$), respectively. R_1-nitro substituted compounds **3c** and **4e** show the lowest inhibitory effect. The decrease in antioxidant activity on LP is related to their electronic distribution and lipophilicity. EC_{50} values of these compounds are 0.087 ± 0.001 and 0.092 ± 0.001 mM ($p < 0.05$), respectively. These results suggest that the indole derivatives may prevent the formation of toxic carbonyl compounds such as lipid peroxides and their aldehyde decomposition products and may play an important role in protection against damage to membrane function.

2.2.2. DPPH radical scavenging activity

Although the DPPH radical scavenging abilities of all the indole derivatives were significantly lower than those of ascorbic acid (0.36 ± 0.04 mM) and α-tocopherol (0.35 ± 0.07 mM), it was evident that they show reducing ability (possibly by hydrogen atom transfer) and could serve as free-radical scavengers. Amongst the **3a** (1.30 ± 0.13 mM), **3c** (1.30 ± 0.10 mM), **4a** (0.98 ± 0.14 mM), **4c** (1.24 ± 0.11 mM), **4d** (1.01 ± 0.15 mM) and **4e** (1.27 ± 0.15 mM), there were no significant differences ($p > 0.05$) in their activities in scavenging DPPH radicals as shown by the small differences of the EC_{50} values (the effective concentration at which the DPPH radicals were scavenged by 50%). The DPPH radical scavenging activities of **3b** and **4b** were comparable ($p > 0.05$) with EC_{50} values of 1.78 ± 0.06 and 1.62 ± 0.06 mM, respectively. These values are significantly higher ($p < 0.05$) than the values observed for the compounds mentioned above, indicating lower scavenging activity.

2.2.3. Total radical antioxidant potential (TRAP)

From the EC_{50} values (the effective concentration at which the ABTS radicals were scavenged by 50%) estimated from the dose–response curves for the compounds, it can be seen that R_1-methyl substituted **3a** (1.02 ± 0.01 mM), R_1-chlorine substituted **3b** (1.03 ± 0.05 mM), R_1-methyl substituted **4a** (0.98 ± 0.14 mM), R_1-chlorine substituted **4c** (1.14 ± 0.14 mM) and R_1-brome substituted **4d** (1.04 ± 0.11 mM) showed similar ($p > 0.05$) degrees of efficacy in their scavenging activities against ABTS radical cation, which were the highest among the tested compounds. The EC_{50} values of these compounds are lower than the values observed for ascorbic acid (1.20 ± 0.03 mM) and α-tocopherol (1.20 ± 0.01 mM). Nevertheless, in R_1-nitro substituted **3c** (1.63 ± 0.04 mM), R_1-trifluoromethoxy substituted **4b** (1.37 ± 0.05 mM) and R_1-nitro substituted **4e** (1.34 ± 0.04 mM) the activity was decreased somewhat when compared with other compounds.

In ABTS radical cation scavenging method, the antioxidant activity of tested compounds was expressed also as the TEAC, the concentration of Trolox solution having an antioxidant activity equivalent to 1 mM concentration of the tested compounds. The TEAC reflects the ability of hydrogen or electron-donating antioxidants to scavenge the ABTS radical cation compared with that of Trolox. TEAC values were found to be 2.01 ± 0.010, 2.02 ± 0.020, 2.04 ± 0.045, 1.95 ± 0.005, 2.00 ± 0.027, 2.07 ± 0.022, 2.06 ± 0.070, 2.00 ± 0.027 and 1.94 ± 0.011 mM Trolox for **3a–c** and **4a–e,** respectively. These values were not significantly different ($p < 0.05$) from that of ascorbic acid (2.13 ± 0.004 mM Trolox) and α-tocopherol (2.02 ± 0.011 mM Trolox) at 3.1 mM.

2.2.4. Reducing power

In the ferric to ferrous reduction assay, the electron donation capacity (reflecting the electron transfer ability) of the compounds was assessed. From the EC_{50} (the effective concentration at which the absorbance was 0.5) it was seen that R_1-chlorine substituted **3b** (0.51 ± 0.11 mM), R_1-methyl substituted **4a** (0.70 ± 0.17 mM), R_1-nitro substituted **3c** (0.80 ± 0.05 mM) and R_1-methyl substituted **3a** (1.36 ± 0.13 mM) showed the highest degree of electron transfer capacity, indicating the highest antioxidant potential amongst all the indole derivatives under study. The capacities of these compounds were generally inferior to ascorbic acid (0.65 ± 0.10 mM), whereas these values are significantly higher than the values observed for α-tocopherol (1.95 ± 0.04 mM) (Table 3). When these data are examined, it is observed that the substitution of the methyl group at R_2 caused significantly decrease in reducing power, whereas in **4a** incorporating methyl both at R_1 and R_2 the activity is 2 times higher than R_1-methyl substituted **3a**. **4b–e** had the lowest reducing powers of 4.94 ± 0.06, 4.02 ± 0.15, 4.22 ± 0.02 and 5.14 ± 0.38, respectively. The data from the iron reduction assay suggests that all the indole derivatives are able to undergo electron transfer to oxidizing species. Therefore, they should be able to reduce reactive radicals as well, converting them into more stable and unreactive species.

2.3. Anticancer activity

Compounds **3b** and **4b** were selected by the National Cancer Institute for screening against anticancer activity. A primary

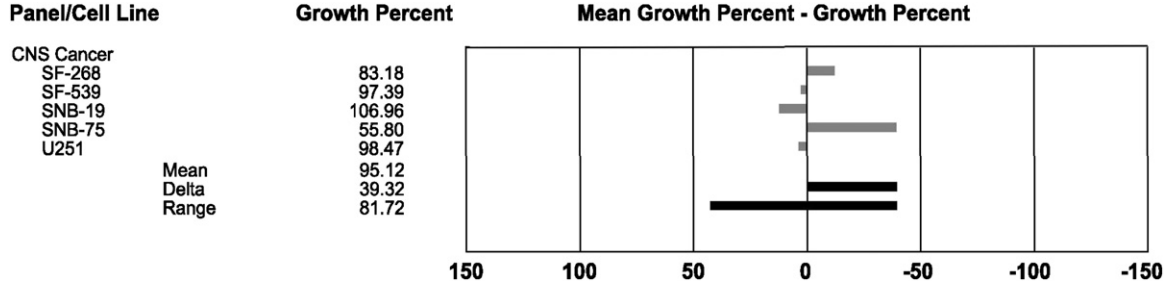

Fig. 6. One dose Mean Graph for CNS cancer cell lines of **3b**.

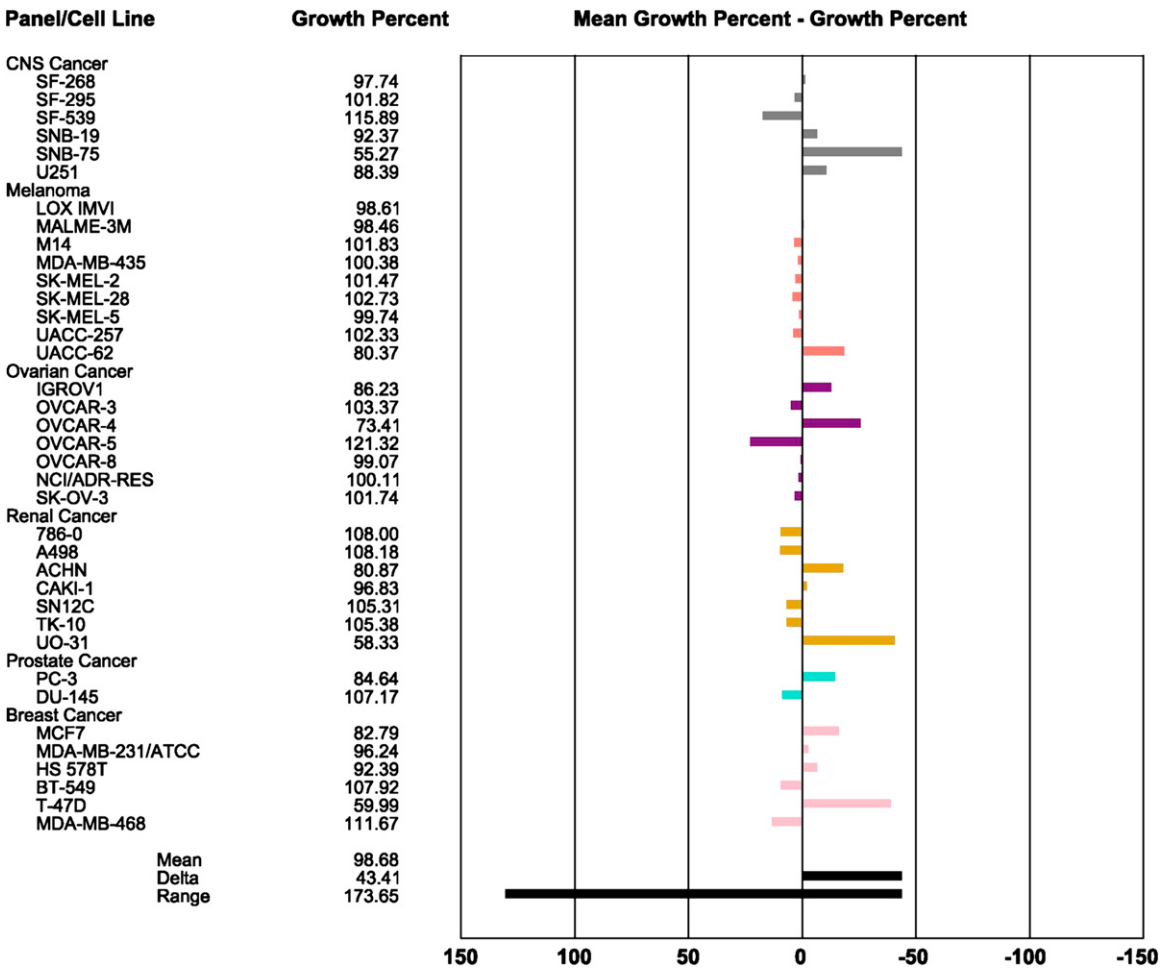

Fig. 7. One dose Mean Graph for CNS cancer, melanoma, ovarian cancer, renal cancer, prostate cancer and breast cancer cell lines of **4b**.

anticancer assay was performed according to the protocol of the Drug Evaluation Branch of the National Cancer Institute, Bethesda [33–36]. The cytotoxic and/or growth inhibitory effects of the compounds were tested *in vitro* at a single dose (10^{-5} M) against the full panel of 60 human tumour cell lines derived from nine neoplastic diseases. The growth percentage was evaluated spectrophotometrically and compared to controls not treated with test agents. A 48 h continuous drug exposure protocol was followed and a sulphorhodamine B (SRB) protein assay was used to estimate cell viability or growth. The cell lines used in the National Cancer Institute screen were leukemia, non-small cell lung cancer (NSCL), colon cancer, central nervous system (CNS) cancer, melanoma, ovarian cancer, renal cancer, prostate cancer and breast cancer cell lines. Mean Graphs were constructed for each effect, with bars depicting the deviation of individual tumour cell lines from the overall mean value for all the cells tested. In the Mean Graph the center point is the mean of all growth inhibition (GI) percentages over all cell lines. Bars that point to the right are cell lines where the inhibition is greater than the average, while bars that point to the left are cell lines where the inhibition is less than the average.

Single dose Mean Graphs of compound **3b** for CNS cancer cell lines and compound **4b** for CNS cancer, melanoma, ovarian cancer, renal cancer, prostate cancer and breast cancer cell lines are shown in Figs. 6 and 7, respectively. For compound **3b,** it was observed that incorporating a chlorine at position 5 of the indole ring, a growth percentage of 55.80% was obtained for a CNS cancer cell line SNB-75. The substitution of the methyl group at position 1 and the trifluoromethoxy group at position 5 of the indole ring caused an increase in cytotoxicity against renal and breast cancer cell lines. For compound **4b**, growth percentages were found to be 55.27% for a CNS cancer cell line SNB-75, 58.33% for a renal cancer cell line UO-31 and 59.99% for a breast cancer cell line T-47D.

3. Conclusion

New spiroindolinones incorporating the benzothiazole moiety were synthesized. The structures were confirmed by elemental analyses, spectrometry and single crystal X-ray analysis. The new compounds were evaluated for antioxidant activity. The results showed that all the indole derivatives had a high degree of potency in inhibiting lipid peroxidation and demonstrated strong scavenging activity against the $DPPH^{\bullet}$ and $ABTS^{\bullet+}$ radicals. Hence, these compounds can be considered as the best antioxidants amongst all. The antioxidant properties increased due to the substitution of the methyl or halogen at R_1 on the spiroindolinones. In fact, among the tested compounds, the most active compounds were **3a**, **3b** and **4a** incorporating methyl or chlorine at R_1. Generally, replacement of these groups at R_1 with trifluoromethoxy or nitro has been found to yield weak active compounds. Interestingly, the substitution of the methyl group at

R_2 caused significantly decrease in reducing power (except **4a**), whereas in the anti-LP, DPPH and ABTS assays, there were only minor variations in activities of R_2-methyl substituted compounds. However, **4a** incorporating methyl both at R_1 and R_2 was found to be the most potent antioxidant described in this study. Although the indole derivatives under study were found to be effective antioxidant candidates in these systems, their potential exploitable beneficial effects and safety in humans need to be proven in clinical trials.

4. Experimental section

4.1. Chemistry

Soybean lecithin (L-α-phosphatidylcholine Type IV-S), 2,2-diphenyl-1-picrylhydrazyl (DPPH$^{\bullet}$), α-tocopherol, ascorbic acid, 5-methylisatin, 5-(trifluorometoxy)isatin, 5-chloroisatin and 5-nitroisatin were purchased from Sigma–Aldrich Chemical Co. (St. Louis, MO, USA). Butylated hydroxytoluene (BHT), 2,2′-azino-bis(3-ethylbenzthiazoline-6-sulphonic acid) (ABTS$^{\bullet+}$) diammonium salt, 6-hydroxy-2,5,7,8,-tetramethylchroman-2-carboxylic acid (Trolox), sodium hydride (NaH), 5-bromoisatin and 2-aminothiophenol were purchased from Fluka Chemical Co. (Bushs, Switzerland). Potassium ferricyanide, thiobarbituric acid (TBA), trichloroacetic acid (TCA), ferric chloride and iodomethane were purchased from Merck (Darmstadt, Germany). All other chemicals used were of analytical grade. Melting points were estimated with a Buchi 540 melting point apparatus in open capillaries and are uncorrected. Elemental analyses were performed on a Thermo Finnigan Flash EA 1112 elemental analyzer. IR spectra were recorded on KBr discs, using a Perkin–Elmer Model 1600 FT-IR spectrometer. ^{1}H NMR and HSQC spectra were obtained on Varian^{UNITY} INOVA 500 spectrophotometers using DMSO-d_6. Mass spectra were determined on an AGILENT 1100 MSD instrument.

4.2. The synthesis of 5-substituted 1-methyl-1H-indole-2,3-diones (**2a–e**)

A suspension of 5-substituted 1*H*-indole-2,3-diones **1a–e** (5 mmol) and NaH (60% suspension in oil) (0.2 g) in anhydrous DMF (5 mL) was stirred for 0.5 h at room temperature. After addition of iodomethane (15 mmol), the mixture was refluxed for 4 h. The product was poured onto ice and water, and then filtered.

4.3. The synthesis of 3H-spiro[1,3-benzothiazole-2,3′-indol]-2′(1′H)-ones (**3a–c**)

To a solution of 5-substituted 1*H*-indole-2,3-diones **1** (3.5 mmol) in ethanol (15 mL) was added 2-aminothiophenol (3.5 mmol). The mixture was refluxed on a water bath for 5 h. The product that was formed after cooling was filtered and recrystallized from ethanol.

4.3.1. 5′-Methyl-3H-spiro[1,3-benzothiazole-2,3′-indol]-2′(1′H)-one (**3a**)

Yellow crystal; yield 74%; m.p. 216 °C; IR (KBr): υ 3299 (NH), 1711 (C=O); ^{1}H NMR (DMSO-d_6, 500 MHz) δ (ppm): 2.25 (s, 3H, ind. 5-CH_3), 6.51 (d, 1H, J = 7.62 Hz, benzothia. C_4–H), 6.61 (dt, 1H, J = 7.63, 1.22 Hz, benzothia. C_6–H), 6.71 (d, 1H, J = 7.93 Hz, ind. C_7–H), 6.89 (dt, 1H, J = 7.62, 1.22 Hz, benzothia. C_5–H), 7.01 (d, 1H, J = 7.62 Hz, benzothia. C_7–H), 7.08 (dd, 1H, J = 7.93, 1.83 Hz, ind. C_6–H), 7.22 (s, 1H, benzothia. NH), 7.36 (d, 1H, J = 0.61 Hz, ind. C_4–H), 10.22 (s, 1H, ind. NH). LCMS-APCI (+) m/z (%): 269 (MH^+, 6), 267 (100). Analyses (%) Calcd for $C_{15}H_{12}N_2OS$ (268.33): C, 67.14; H, 4.51; N, 10.44. Found: C, 67.00; H, 4.35; N, 10.47.

4.3.2. 5′-Chloro-3H-spiro[1,3-benzothiazole-2,3′-indol]-2′(1′H)-one (**3b**)

Yellow crystal; yield 60%; m.p. 219 °C; IR (KBr): υ 3302 (NH), 1714 (C=O); ^{1}H NMR (DMSO-d_6, 500 MHz) δ (ppm): 6.54 (d, 1H, J = 7.58 Hz, benzothia. C_4–H), 6.63 (t, 1H, J = 7.63 Hz, benzothia. C_6–H), 6.85 (d, 1H, J = 8.23 Hz, ind. C_7–H), 6.91 (dt, 1H, J = 7.63, 1.22 Hz, benzothia. C_5–H), 7.04 (d, 1H, J = 7.32 Hz, benzothia. C_7–H), 7.28 (s, 1H, benzothia. NH), 7.33 (dd, 1H, J = 8.23, 2.13 Hz, ind. C_6–H), 7.52 (d, 1H, J = 2.14 Hz, ind. C_4–H), 10.48 (s, 1H, ind. NH). LCMS-APCI (+) m/z (%): 289 (MH^+, 40), 287 (100). Analyses (%) Calcd for $C_{14}H_9ClN_2OS$ (288.75): C, 58.23; H, 3.14; N, 9.70. Found: C, 58.34; H, 2.78; N, 9.59.

4.3.3. 5′-Nitro-3H-spiro[1,3-benzothiazole-2,3′-indol]-2′(1′H)-one (**3c**)

Orange powder; yield 71%; m.p. 212–3 °C; IR (KBr): υ 3354 (NH), 1732 (C=O); ^{1}H NMR (DMSO-d_6, 500 MHz) δ (ppm): 6.61 (d, 1H, J = 7.99 Hz, benzothia. C_4–H), 6.69 (t, 1H, J = 7.68 Hz, benzothia. C_6–H), 6.95 (t, 1H, J = 7.67 Hz, benzothia. C_5–H), 7.07 (d, J = 8.63 Hz, ind. C_7–H), 7.10 (d, 1H, J = 7.35 Hz, benzothia. C_7–H), 7.33 (s, 1H, benzothia. NH), 8.25 (dd, 1H, J = 8.63, 2.24 Hz, ind. C_6–H), 8.27 (d, 1H, J = 2.24 Hz, ind. C_4–H), 11.07 (s, 1H, ind. NH). Analyses (%) Calcd for $C_{14}H_9N_3O_3S$ (299.30): C, 56.18; H, 3.03; N, 14.04. Found: C, 56.20; H, 3.03; N, 13.63.

4.4. The synthesis of 1′-methyl-3H-spiro[1,3-benzothiazole-2,3′-indol]-2′(1′H)-ones (**4a–e**)

To a solution of 5-substituted 1-methyl-1*H*-indole-2,3-diones **2** (3.5 mmol) in ethanol (15 mL) was added 2-aminothiophenol (3.5 mmol). The mixture was refluxed on a water bath for 5 h. The product formed after cooling was filtered and recrystallized from ethanol.

4.4.1. 1′,5′-Dimethyl-3H-spiro[1,3-benzothiazole-2,3′-indol]-2′-one (**4a**)

Brown powder; yield 41%; m.p. 182–3 °C; IR (KBr): υ 3303 (NH), 1696 (C=O); ^{1}H NMR (DMSO-d_6, 500 MHz) δ (ppm): 2.28 (s, 3H, ind. 5-CH_3), 3.08 (s, 3H, N–CH_3), 6.52 (d, 1H, J = 7.32 Hz, benzothia. C_4–H), 6.63 (t, 1H, J = 7.32 Hz, benzothia. C_6–H), 6.90 (dt, J = 7.62, 1.22 Hz, 1H, benzothia. C_5–H), 6.92 (d, J = 7.93 Hz, 1H, ind. C_7–H), 7.03 (dd, J = 7.62, 1.22 Hz, 1H, benzothia. C_7–H), 7.18 (d, 2H, J = 7.80 Hz, ind. C_6–H, benzothia. NH), 7.41 (s, 1H, ind. C_4–H). HSQC (DMSO-d_6) δ (ppm): 21.19 (ind. 5-CH_3), 26.91 (N–CH_3), 74.80 (spiro C), 109.17 (benzothia. C_4), 109.46 (ind. C_7), 119.40 (benzothia. C_6), 121.74 (benzothia. C_7), 124.77 (ind. C_{3a}), 126.41 (ind. C_4), 126.46 (benzothia. C_5), 130.04 (ind. C_5), 131.43 (ind. C_6), 132.96 (benzothia. C_{7a}), 141.04 (ind. C_{7a}), 147.68 (benzothia. C_{3a}), 175.12 (ind. C_2). Analyses (%) Calcd for $C_{16}H_{14}N_2OS$ (282.36): C, 68.06; H, 5.00; N, 9.92. Found: C, 68.14; H, 5.13, N, 9.57.

4.4.2. 1′-Methyl-5′-trifluoromethoxy-3H-spiro[1,3-benzothiazole-2,3′-indol]-2′-one (**4b**)

Yellow crystal; yield 39%; m.p. 187–9 °C; IR (KBr): υ 3307 (NH), 1703 (C=O); ^{1}H NMR (DMSO-d_6, 500 MHz) δ (ppm): 3.13 (s, 3H, N–CH_3), 6.58 (d, 1H, J = 7.93 Hz, benzothia. C_4–H), 6.66 (dt, 1H, J = 7.62, 1.22 Hz, benzothia. C_6–H), 6.93 (dt, 1H, J = 7.87, 1.22 Hz, benzothia. C_5–H), 7.06 (d, 1H, J = 8.54 Hz, ind. C_7–H), 7.15 (d, J = 7.86 Hz, benzothia. C_7–H), 7.28 (s, 1H, benzothia. NH), 7.42 (dd, 1H, J = 8.54, 1.83 Hz, ind. C_6–H), 7.55 (d, 1H, J = 2.44 Hz, ind. C_4–H). HSQC (DMSO-d_6) δ (ppm): 27.11 (N–CH_3), 74.55 (spiro C), 109.43 (benzothia. C_4), 110.97 (benzothia. C_7), 119.34 (ind. C_4), 119.71 (benzothia. C_6), 120.85 (CF_3O), 121.89 (ind. C_7), 124.45 (ind. C_{3a}), 124.58 (ind. C_6), 126.59 (benzothia. C_5), 131.93 (ind. C_{7a}), 142.64 (benzothia. C_{7a}), 144.77 (ind. C_5), 147.38 (benzothia. C_{3a}), 175.18 (ind. C_2). LCMS-APCI (+) m/z (%): 353 (MH^+, 100). Analyses (%) Calcd for

$C_{16}H_{11}F_3N_2O_2S$ (352.33): C, 54.54; H, 3.15; N, 7.95. Found: C, 54.91; H, 3.08; N, 8.01.

4.4.3. 5′-Chloro-1′-methyl-3H-spiro[1,3-benzothiazole-2,3′-indol]-2′-one (**4c**)

Dark yellow powder; yield 46%; m.p. 166 °C; IR (KBr): υ 3307 (NH), 1698 (C═O); ^{1}H NMR (DMSO-d_6, 500 MHz) δ (ppm): 3.10 (s, 3H, N–CH_3), 6.56 (d, 1H, J = 7.93 Hz, benzothia. C_4–H), 6.65 (t, 1H, J = 7.47 Hz, benzothia. C_6–H), 6.92 (dt, 1H, J = 7.62, 1.22 Hz, benzothia. C_5–H), 7.07 (d, 1H, J = 8.23 Hz, ind. C_7–H), 7.07 (d, 1H, J = 7.32 Hz, benzothia. C_7–H), 7.25 (s, 1H, benzothia. NH, D_2O exchange), 7.45 (dd, 1H, J = 8.23, 2.13 Hz, ind. C_6–H), 7.57 (d, 1H, J = 2.12 Hz, ind. C_4–H). HSQC (DMSO-d_6) δ (ppm): 27.08 (N–CH_3), 74.56 (spiro C), 109.45 (benzothia. C_4), 111.43 (ind. C_7), 119.71 (benzothia. C_6), 121.89 (benzothia. C_7), 124.54 (ind. C_{3a}), 125.77 (ind. C_4), 126.57 (benzothia. C_5), 127.75 (ind. C_5), 131.07 (ind. C_6), 132.12 (benzothia. C_{7a}), 142.34 (ind. C_{7a}), 147.40 (benzothia. C_{3a}), 174.88 (ind. C_2). Analyses (%) Calcd for $C_{15}H_{11}ClN_2OS$ (302.77): C, 59.50; H, 3.66; N, 9.25. Found: C, 59.36; H, 4.03; N, 9.19.

4.4.4. 5′-Bromo-1′-methyl-3H-spiro[1,3-benzothiazole-2,3′-indol]-2′-one (**4d**)

Orange crystal; yield 53%; m.p. 244–6 °C; IR (KBr): υ 3327 (NH), 1719 (C═O); ^{1}H NMR (DMSO-d_6, 500 MHz) δ (ppm): 3.10 (s, 3H, N–CH_3), 6.56 (d, 1H, J = 7.32 Hz, benzothia. C_4–H), 6.65 (t, 1H, J = 7.32 Hz, benzothia. C_6–H), 6.92 (t, 1H, J = 7.32 Hz, benzothia. C_5–H), 7.03 (d, 1H, J = 8.29 Hz, ind. C_7–H), 7.06 (d, 1H, J = 7.32 Hz, benzothia. C_7–H), 7.25 (s, 1H, benzothia. NH), 7.58 (dd, 1H, J = 8.30, 1.95 Hz, ind. C_6–H), 7.67 (d, 1H, J = 1.95 Hz, ind. C_4–H). HSQC (DMSO-d_6) δ (ppm): 27.07 (N–CH_3), 74.51 (spiro C), 109.45 (benzothia. C_4), 111.93 (ind. C_7), 115.30 (ind. C_5), 119.72 (benzothia. C_6), 121.90 (benzothia. C_7), 124.53 (ind. C_{3a}), 126.58 (benzothia. C_5), 128.46 (ind. C_4), 132.46 (benzothia. C_{7a}), 133.93 (ind. C_6), 142.35 (ind. C_{7a}), 147.37 (benzothia. C_{3a}), 174.75 (ind. C_2). Analyses (%) Calcd for $C_{15}H_{11}BrN_2OS$ (347.22): C, 51.89; H, 3.19; N, 8.07. Found: C, 52.12; H, 3.59; N, 8.06.

4.4.5. 1′-Methyl-5′-nitro-3H-spiro[1,3-benzothiazole-2,3′-indol]-2′-one (**4e**)

Red powder; yield 75%; m.p. 211 °C; IR (KBr): υ 3348 (NH), 1727 (C═O); ^{1}H NMR (DMSO-d_6, 500 MHz) δ (ppm): 3.20 (s, 3H, N–CH_3), 6.61 (d, 1H, J = 7.80 Hz, benzothia. C_4–H), 6.69 (t, 1H, J = 7.32 Hz, benzothia. C_6–H), 6.95 (dt, 1H, J = 7.81, 1.47 Hz, benzothia. C_5–H), 7.10 (d, 1H, J = 7.81 Hz, benzothia. C_7–H), 7.27 (s, 1H, benzothia. NH), 7.29 (d, J = 8.79 Hz, ind. C_7–H), 8.29 (d, 1H, J = 2.44 Hz, ind. C_4–H), 8.34 (dd, 1H, J = 8.78, 2.44 Hz, ind. C_6–H). HSQC (DMSO-d_6) δ (ppm): 27.48 (N–CH_3), 74.10 (spiro C), 109.74 (benzothia. C_4), 110.35 (ind. C_7), 120.02 (benzothia. C_6), 120.90 (ind. C_4), 122.04 (benzothia. C_7), 124.35 (ind. C_{3a}), 126.74 (benzothia. C_5), 128.13 (ind. C_6), 131.41 (benzothia. C_{7a}), 143.78 (ind. C_5), 147.07 (benzothia. C_{3a}), 149.39 (ind. C_{7a}), 175.62 (ind. C_2). Analyses (%) Calcd for $C_{15}H_{11}N_3O_3S$ (313.33): C, 57.50; H, 3.54; N, 13.41. Found: C, 57.61; H, 2.91; N, 13.60.

4.5. Single crystal X-ray structure determination

Crystal of **4d** of suitable quality and size, was mounted on the ends of glass and used for the intensity data collection. X-ray crystallographic measurements were carried out using an STOE IPDS 2 single crystal diffractometer equipped with image plate detector. Graphite monochromated MoKα radiation (λ = 0.71073 Å) was generated at 50 kV and 40 mA. The cell parameters and the orientation matrices for data collection were obtained from a least-squares refinement using the setting angles of 10,163 carefully centered reflections in the range $1.52 < \theta < 26.1°$. A total of 7792 reflections were collected. Data was corrected for Lorentz-polarisation effects and for absorption using empirical integration method.

The structure of **4d** was solved by direct methods program SHELXS-97 [37] and refined by the full-matrix least-squares method based on F^2 using SHELXL-97 [38]. All non-hydrogen atoms were refined with anisotropic displacement factors. The H atom of N_2 was found in the difference Fourier map, and its position and isotropic thermal parameters were refined; remaining hydrogen atoms were positioned geometrically and refined using a riding model. The geometric calculations were carried out with the Platon [39] program.

4.6. In vitro evaluation of antioxidant activity

4.6.1. Antioxidant activity on liposome peroxidation

The antioxidative effects of indole derivatives were quantified by using the inhibition of the Fe^{3+}/ascorbate induced lipid peroxidation in liposomes. Phosphatidylcholine (lecithin), a phospholipid believed to be present in high amounts in cell membranes, was used a liposome-like substrate.

The lipid peroxidation assay was based on the method described by Duh et al. [40]. Lecithin (300 mg) was suspended in 30 mL phosphate buffer (10 mmol/L, pH 7.4). This suspension was sonicated with a rod using an ultrasonic homogenizer (Bandelin, Berlin, Germany) at 30 s intervals for 10 min until an opalescent suspension was obtained.

The sonicated solution (10 mg/mL), $FeCl_3$, ascorbic acid and the indole derivatives (0.025–0.4 mM) or the reference antioxidant α-tocopherol (0.1–0.4 mM) were mixed to produce a final concentration of 3.08 mg liposome/mL, 123.2 μmol $FeCl_3$ and 123.2 μmol ascorbic acid. After 1 h incubation at 37 °C, the formation of lipid peroxidation products was assayed by the measurement of malondialdehyde (MDA) levels on the basis that MDA reacted with TBA at 532 nm according to Buege and Aust [41]. Briefly, 500 μL of this reaction mixture was mixed with 1000 μL TCA–TBA reagent (consisting of 15% w/v TCA and 0.375% TBA in 0.25 N HCl) and 14 μL butylated hydroxytoluene (BHT) (2% in absolute ethanol). The mixture was vortexed and heated for 10 min in a boiling water bath. After cooling, an equal volume of n-butanol was added and the mixture was shaken vigorously. The n-butanol layer was separated by centrifugation at 3000 rpm for 5 min. The absorbance of the sample was measured at 532 nm against a blank, which contained all reagents except lecithin. The percentage inhibition of lipid peroxidation was calculated by comparing the results of the samples with those of controls not treated with the extract using the following equation: Inhibition effect (%) = [1 − (Absorbance of sample at 532 nm/Absorbance of control at 532 nm)] × 100.

4.6.2. DPPH radical scavenging activity

The DPPH radical scavenging activities of the indole derivatives were measured according to the procedure described by Brand-Williams et al. [42]. A purple-colored (DPPH$^•$), is a stable free radical, which is reduced to DPPH (yellow colored) by reacting with an antioxidant. A 0.1 mL aliquot of each indole derivatives (0.2–6.25 mM) in DMSO, ascorbic acid (0.1–0.8 mM) or α-tocopherol (0.1–0.8 mM) in absolute ethanol was added to 3.9 mL of 6×10^{-5} M methanolic solution of DPPH. The mixture was shaken vigorously and allowed to stand in the dark at room temperature for 30 min. The decrease in absorbance of the resulting solution was then measured spectrophotometrically at 517 nm against methanol. All measurements were made in triplicate and averaged. Two controls were used for this test, a negative control (containing all reagents except the test sample) and positive controls (using the reference antioxidants). The ability to scavenge DPPH radical was calculated by the following equation: DPPH radical scavenging

activity (%) = [1 − (Absorbance of sample at 517 nm/Absorbance of control at 517 nm)] × 100.

4.6.3. Total radical antioxidant potential (TRAP)

The total radical antioxidant potential of indole derivatives was measured using TEAC assay as described by Re et al. [43] with minor modifications.

After addition of 990 μL of $ABTS^{\bullet+}$ solution to 10 μL of indole derivatives (0.2–6.25 mM), ascorbic acid (0.2–3.1 mM), α-tocopherol (0.2–3.1 mM) or Trolox standards (final concentration 0–20 μM in ethanol), the decrease in absorbance at 734 nm was monitored exactly 6 min after the initial mixing. Appropriate ethanol blanks were run in each assay. All determinations were carried out in triplicate. The ability to scavenge $ABTS^{\bullet+}$ radical was calculated by the following equation: ABTS radical scavenging activity (%) = [1 − (Absorbance of sample at 734 nm/Absorbance of control at 734 nm)] × 100.

4.6.4. Reducing power

The reducing powers of the indole derivatives, ascorbic acid and α-tocopherol were determined according to the method described by Chung, et al. [44]. A 0.1 mL aliquot of each indole derivative (1.6–6.25 mM), ascorbic acid (0.4–3.1 mM) or α-tocopherol (0.4–6.25 mM) were mixed with an equal volume of 0.2 M phosphate buffer (pH 6.6) and 1% potassium ferricyanide, and then incubated at 50 °C for 20 min 0.25 mL of 1% trichloroacetic acid was added to the mixture to stop the reaction, and then the mixture was centrifuged at 2790 g for 10 min. The supernatant (0.25 mL) was mixed with 0.25 mL of distilled water and 0.1% of $FeCl_3$ (0.5 mL) and then the absorbance was measured at 700 nm. The reducing powers of the tested samples increased with the absorbance values.

4.6.5. Statistical analysis

Results were expressed as the mean ± the standard deviation (SD) of triplicate analysis. Statistical comparisons were performed using the Student's *t*-test. Differences were considered significant at $p < 0.05$.

4.7. In vitro evaluation of cancer activity

The human tumour cell lines of the cancer screening panel were grown in RPMI 1640 medium containing 5% fetal bovine serum and 2 mM L-glutamine. For a typical screening experiment, cells were inoculated into 96 well microtiter plates in 100 μL at plating densities ranging from 5000 to 40,000 cells/well depending on the doubling time of individual cell lines. After cell inoculation, the microtiter plates were incubated at 37 °C, 5% CO_2, 95% air and 100% relative humidity for 24 h prior to addition of experimental drugs. After 24 h, two plates of each cell line were fixed *in situ* with trichloroacetic acid (TCA), to represent a measurement of the cell population for each cell line at the time of drug addition (Tz). Experimental drugs were solubilized in dimethyl sulfoxide at 400-fold the desired final maximum test concentration and stored frozen prior to use. At the time of drug addition, an aliquot of frozen concentrate was thawed and diluted to twice the desired final maximum test concentration with complete medium containing 50 μg/mL gentamicin. Additional four, 10-fold or 0.5 log serial dilutions were made to provide a total of five drug concentrations plus control. Aliquots of 100 μL of these different drug dilutions were added to the appropriate microtiter wells already containing 100 μL of medium, resulting in the required final drug concentrations. Following drug addition, the plates were incubated for an additional 48 h at 37 °C, 5% CO_2, 95% air, and 100% relative humidity. For adherent cells, the assay was terminated by the addition of cold TCA. Cells were fixed *in situ* by the gentle addition of 50 μL of cold 50% (w/v) TCA (final concentration, 10% TCA) and incubated for 60 min at 4 °C. The supernatant was discarded, and the plates were washed five times with tap water and air-dried. Sulphorhodamine B (SRB) solution (100 μL) at 0.4% (w/v) in acetic acid was added to each well, and plates were incubated for 10 min at room temperature. After staining, unbound dye was removed by washing five times with 1% acetic acid and the plates were air-dried. Bound stain was subsequently solubilized with 10 mM trizma base, and the absorbance was measured on an automated plate reader at a wavelength of 515 nm. For suspension cells, the methodology was the same except that the assay was terminated by fixing settled cells at the bottom of the wells by gently adding 50 μL of 80% TCA (final concentration, 16% TCA). Using the seven absorbance measurements [time zero, (Tz), control growth, (C), and test growth in the presence of drug at the five concentration levels (Ti)], the percentage growth was calculated at each of the drug concentrations levels. The percentage growth inhibition was calculated as:

$$[(Ti - Tz)/(C - Tz)] \times 100 \text{ for concentrations for which } Ti \geq Tz$$

$$[(Ti - Tz)/Tz] \times 100 \text{ for concentrations for which } Ti < Tz$$

Acknowledgements

We thank the Drug Research and Development, Division of Cancer Research, National Cancer Institute, Bethesda, Maryland, for the anticancer activity screening of the compounds. This work was supported by Istanbul University Research Fund, Projects Number: BYP-1895.

References

[1] C.J. Valko, J. Rhodes, M. Moncol, M. Izakovic, M. Mazur, Chemico-Biol. Int. 160 (2006) 1–40.
[2] W. Dröge, Physiol. Rev. 82 (2002) 47–95.
[3] D. Venkat Ratnam, D.D. Ankola, V. Bhardwaj, D.K. Sahana, M.N.V. Ravi Kumar, J. Control. Release 113 (2006) 189–207.
[4] S. Süzen, Top. Heterocycl. Chem. 11 (2007) 145–178.
[5] H.Y. Aboul-Enein, A. Kladna, I. Kruk, K. Lichszteld, T. Michalska, S. Olgen, Biopolymers 78 (2005) 171–178.
[6] S. Ölgen, Z. Kılıç, A.O. Ada, T. Çoban, J. Enz. Inhib. Med. Chem. 22 (2007) 457–462.
[7] S. Ölgen, P. Varol, T. Çoban, D. Nebioğlu, J. Enz. Inhib. Med. Chem. 23 (2008) 334–340.
[8] Z. Ateş-Alagöz, C. Kuş, T. Çoban, J. Enz. Inhib. Med. Chem. 20 (2005) 325–331.
[9] R. Mezencev, J. Mojžiš, M. Pilátová, P. Kutschy, Neoplasma 50 (2003) 239–245.
[10] M. Pilátová, M. Šarišský, P. Kutschy, A. Mirošsay, R. Mezencev, Z. Čurillová, M. Suchý, K. Monde, L. Mirossay, J. Mojžiš, Leuk. Res. 29 (2005) 415–421.
[11] R. Mezencev, P. Kutschy, A. Saloyová, Z. Čurillová, J. Mojzis, M. Pilátová, J. McDonald, Chemotherapy 54 (2008) 372–378.
[12] P. Kutschy, A. Saloyová, Z. Čurillová, T. Kožár, R. Mezencev, J. Mojžiš, M. Pilátová, E. Balentová, P. Pazdera, M. Sabol, M. Zburová, Bioorg. Med. Chem. 17 (2009) 3698–3712.
[13] C.G. Mortimer, G. Wells, J.-P. Crochard, E.L. Stone, T.D. Bradshaw, M.F.G. Stevens, A.D. Westwell, J. Med. Chem. 49 (2006) 179–185.
[14] S.H.L. Kok, H.C. Chui, W.S. Lam, J. Chen, F.Y. Lau, R.S.M. Wong, G.Y.M. Cheng, P.B.S. Lai, T.W.T. Leung, M.W.Y. Yu, J.C.O. Tang, A.S.C. Chan, Bioorg. Med. Chem. Lett. 17 (2007) 1155–1159.
[15] I. Čaleta, M. Kralj, M. Marjanović, B. Bertoša, S. Tomić, G. Pavlović, K. Pavelić, G. Karminski-Zamola, J. Med. Chem. 52 (2009) 1744–1756.
[16] M.J. De Brabander, A.S. Josephine, J.E.M.F. Leysen, PCT Int. Appl.. (1996), WO 9625931 A2 19960829.
[17] J. Singh, M.E. Gurney, B. Alex, A. Kiselyov, M. Rao, US Patent Appl. (2009), WO 275164 A1 20090130076.
[18] A. Ben-Alloum, S. Bakkas, M. Soufiaoui, Tetrahedron Lett. 38 (1997) 6395–6396.
[19] R.H. Tale, Org. Lett. 4 (2002) 1641–1642.
[20] K.C. Joshi, A. Dandia, S. Khanna, Indian J. Chem. Soc. 29B (1990) 824–829.
[21] A. Dandia, S. Khanna, K.C. Joshi, J. Indian Chem. Soc. 67 (1990) 824–826.
[22] J.F.M. Da-Silva, S.J. Garden, A.C. Pinto, J. Braz. Chem. Soc. 12 (2001) 273–324.
[23] Y.A. Alam, G.A.M. Nawwar, Heteroatom Chem. 13 (2002) 207–210.
[24] I. Petrov, O. Grupce, T. Stafilov, J. Mol. Struct. 142 (1986) 275–278.
[25] A. Castiñeiras, M.C. Gómez, P. Sevillano, J. Mol. Struct. 554 (2000) 301–306.
[26] P. Naumov, F. Anastasova, Spectrochim. Acta Part A 57 (2001) 469–481.
[27] H. Laatsch, R.H. Thomson, P.J. Cox, J. Chem. Soc. Perkin. Trans. II (1984) 1331–1340.

[28] J. Jayashankaran, R.D.R.S. Manian, R. Raghunathan, Tetrahedron Lett. 45 (2004) 7303–7305.
[29] E.C. Angell, D.C. Black, N. Kumar, Magn. Reson. Chem. 30 (1992) 1–5.
[30] V.S. Hegde, G.D. Kolavi, R.S. Lamani, I.A.M. Khazi, J. Sulfur Chem. 27 (2006) 553–569.
[31] S. Billeau, F. Chatel, M. Robin, R. Faure, J.-P. Galy, Magn. Reson. Chem. 44 (2006) 102–105.
[32] D. Cremer, J.A. Pople, J. Am. Chem. Soc. 97 (1975) 1354–1358.
[33] M.C. Alley, D.A. Scudiero, P.A. Monks, M.L. Hursey, M.J. Czerwinski, D.L. Fine, B.J. Abbott, J.G. Mayo, R.H. Shoemaker, M.R. Boyd, Cancer Res. 48 (1988) 589–601.
[34] M.R. Grever, S.A. Schepartz, B.A. Chabner, The National Cancer Institute: cancer drug discovery and development program. Semin. Oncol. 19 (1992) 622–638.
[35] M.R. Boyd, K.D. Paull, Drug Dev. Res. 34 (1995) 91–109.
[36] R.H. Shoemaker, Nat. Rev. Cancer 6 (2006) 813–823.
[37] G.M. Sheldrick, SHELXS97. Program for Crystal Structure Solution. University of Göttingen, Germany, 1997.
[38] G.M. Sheldrick, SHELXL97. Program for Crystal Structure Refinement. University of Göttingen, Germany, 1997.
[39] A.L. Spek, PLATON. A Multipurpose Crystallographic Tool. Utrecht University, Utrecht, The Netherlands, 2003.
[40] P.-D. Duh, Y.-Y. Tu, G.-C. Yen, Leben.-Wiss. Technol. Food Sci. Technol. 32 (1999) 269–277.
[41] J.A. Buege, S.D. Aust, Meth. Enzymol. 52 (1978) 302–310.
[42] W. Brand-Williams, M.E. Cuvelier, C. Berset, Leben.-Wiss. Technol. Food Sci. Technol. 28 (1995) 25–30.
[43] R. Re, N. Pellegrini, A. Proteggente, A. Pannala, M. Yang, M.C. Rice-Evans, Free Radic. Biol. Med. 26 (1999) 1231–1237.
[44] Y.-C. Chung, S.-J. Chen, C.-K. Hsu, C.-T. Chang, S.-T. Chou, Food Chem. 91 (2005) 419–424.